Wake measurement of utility-scale wind turbine wake using drone

Uchida, Takanori
Research Institute for Applied Mechanics (RIAM), Kyushu University

Takakuwa, Susumu
ENEOS Renewable Energy Corporation

Murakami, Reo
Tokyo Gas Co., Ltd.

出版情報：Journal of Physics: Conference Series. 3016, pp.012015-, 2025-05-01. IOP Publishing
バージョン：

Wake measurement of utility-scale wind turbine wake using drone

Journal of Physics: Conference Series **3016** (2025) 012015 doi:10.1088/1742-6596/3016/1/012015

Wake measurement of utility-scale wind turbine wake using drone

Takanori Uchida[1*], Susumu Takakuwa[2] and Reo Murakami[3]

[1] Research Institute for Applied Mechanics (RIAM), Kyushu University, 6-1 Kasuga-kouen, Kasuga, Fukuoka 816-8580, Japan
[2] ENEOS Renewable Energy Corporation, Roppongi Hills North Tower 10F, 6-2-31 Roppongi, Minato-ku, Tokyo, 106-0032, Japan
[3] Tokyo Gas Co., Ltd., 1-5-20 Kaigan, Minato-ku, Tokyo 105-8527, Japan

[*]E-mail: takanori@riam.kyushu-u.ac.jp

Abstract. In this study, we investigated a method of utilizing the drone itself as a wind speed sensor without mounting a special observation device on the drone. As a result, we constructed a calibration formula to convert the flight record data to an arbitrary wind speed. Next, we applied this method to the airflow measurement in the wake region for the utility-scale wind turbine and succeeded in reproducing the airflow characteristics caused by the wind turbine wake phenomenon.

1. Introduction

In recent years, small unmanned aerial vehicles (UAVs, commonly known as drones) have undergone rapid technological innovation and are expanding their range of applications in various fields such as agriculture, transportation, and surveying. Its use is rapidly progressing in the field of weather observation as well. Compared to existing observation methods that use weather observation towers or Doppler lidar (remote sensing technology), drones' greatest strengths are that they are extremely easy to move and can perform weather observations at low cost without depending on the ground surface coverage. However, most of the cases reported so far have been carried out using observation equipment mounted on a drone.

In this study, we attempt a method to utilize the quadcopter structure-type drone itself as a wind speed sensor without installing special observation equipment on the drone [1)]. In other words, it utilizes flight record data stored on the drone itself. In this study, we first conducted a calibration test for using a drone as a wind speed sensor using a large wind tunnel facility (test section: 15m long x 3.6m wide x 2m high, turbulence intensity in the main flow direction is 0.5% or less) owned by the Research Institute of Applied Mechanics (RIAM), Kyushu University. Next, we attempted to measure the airflow within the wake region of the utility-scale wind turbine on a full scale [2, 3)].

2. Overview of drone calibration tests in the large wind tunnel facility

In this study, the drone was kept constantly hovering. We developed a method to extract characteristic variables from the flight record data obtained at that time and calculate wind speed based on them. In this study, we used a quadcopter-type drone with four rotors. When a drone hovers in the air, it balances with rotor thrust, wind resistance, and gravity (Figure 1).

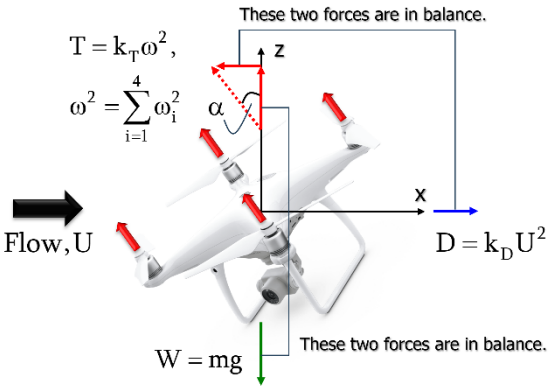

Figure 1. Balance of forces acting on the drone

Here, using the rotor rotational speed ω_i, we define its square value $\omega^2 = \sum_{i=1}^{4} \omega_i^2$. Furthermore, we assume that thrust proportional to rotational speed. The balance of forces acting on the drone is described as shown in Figure 1. From which, the following relational expression regarding the horizontal wind speed U can be obtained. Here, α is the slope angle, and k_T and k_D are nonlinear coefficients.

$$U^2 = \frac{k_T}{k_D}\omega^2 \sin\alpha$$

From the above, we were able to associate the square value of the wind speed that we wanted to find with the variables made up of the drone's rotor rotational speed and tilt angle. In this study, we calculated the wind speed when the drone was hovering based on an arbitrary $\omega^2\sin\alpha$. In other words, it is an image of a hovering drone performing fixed-point observation. In this study, we used two commercially available drones, DJI Phantom 4 Advanced (abbreviation: P4A) and Phantom 4 Pro (abbreviation: P4P), shown in Figure 2.

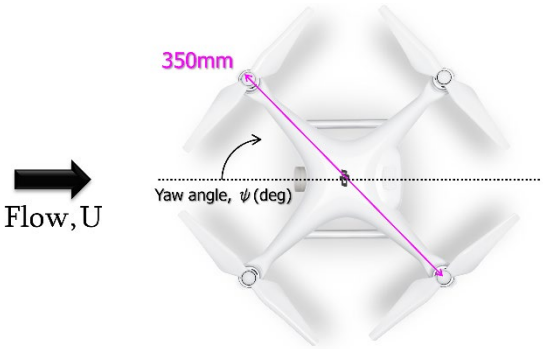

Figure 2. Drone used in this study (DJI Phantom 4 Advanced/Pro)

The two models used in this study have almost the same performance, and various numerical information such as the altitude above ground level during flight, motor and battery information, and the latitude and longitude of the flight are recorded as flight record data. The drone used in this study has two types of functions (indoor/outdoor) that autonomously control its altitude and

hover stably even when subjected to external forces. We used an indoor method called VPS (Visual Positioning system) inside the wind tunnel. This method performs stable hovering based on image recognition using a small camera sensor installed inside the drone. In this study, we created markers for image recognition on the wind tunnel floor to enable stable hovering. In addition, to prevent damage to the wind tunnel when the drone flies away, the drone and the wind tunnel floor were tied together with string, as shown in Figure 3. Furthermore, in order to minimize the influence of the blockage effect, we removed part of the left and right side walls and the top plate of the test section and installed a net there. The wind speed range during calibration is U = 0 to 10m/s. Regarding the yaw angle of the drone, we set $\psi = 0°$ when facing the wind direction, as shown in Figure 2. On the other hand, during the wake measurement for the utility-scale wind turbine, which will be described later, stable hovering was achieved by using GPS (Global Positioning System) signals.

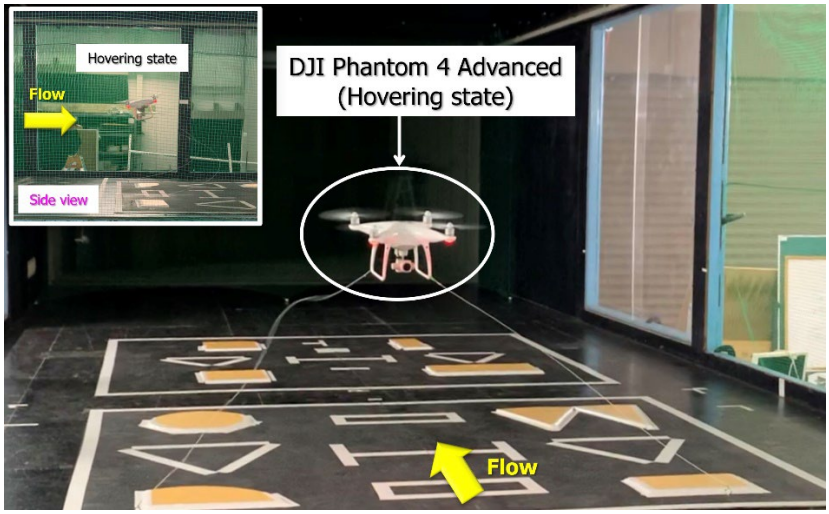

Figure 3. Calibration of a drone using a large boundary layer wind tunnel, U=10m/s

3. Drone calibration test results in the wind tunnel and considerations

In this study, as shown in Figure 3, a drone was hovered in the center of the wind tunnel test section, and each data was acquired by increasing the wind speed in stages (U = 0 to 10m/s). Figure 4 shows the temporal change of $\omega^2\sin\alpha$. It was confirmed that the drone used in this study can hover stably at wind speeds up to 10m/s. Based on Figure 4, we extracted the hovering portion at each wind speed and created a new graph of U^2 and $\omega^2\sin\alpha$. Here, $\omega^2\sin\alpha$ indicates the average value for hovering period. As a result, we obtained a calibration curve from only two variables, U^2 and $\omega^2\sin\alpha$, and calculated the wind speed U corresponding to any $\omega^2\sin\alpha$.

Before conducting wake measurements on the utility-scale wind turbine, in this study we generated a pulsating flow that periodically fluctuated at U = 3 to 8m/s in a wind tunnel to verify the effectiveness of airflow measurements using a drone. The obtained results are shown in Figure 6. The wind speed values calculated by the drone were compared with the results of an ultrasonic anemometer (abbreviated as USA) installed in the wind tunnel test section. It was shown that the drone measurement results shown by the red dotted line closely reproduced the measurement results from the USA shown by the black solid line. If the wind speed suddenly increases to 8m/s, the VPS will no longer function stably and the drone itself will be swept

downstream of the test section. As a result, the operator had to make fine adjustments to the drone's position inside wind tunnel. Finally, the measurements at a wind speed of 8m/s showed slight fluctuations and an underestimation of the average value due to the vibration of the drone itself. Outdoor wake measurements based on GPS signals did not reveal any vibrations of the drone itself as described above.

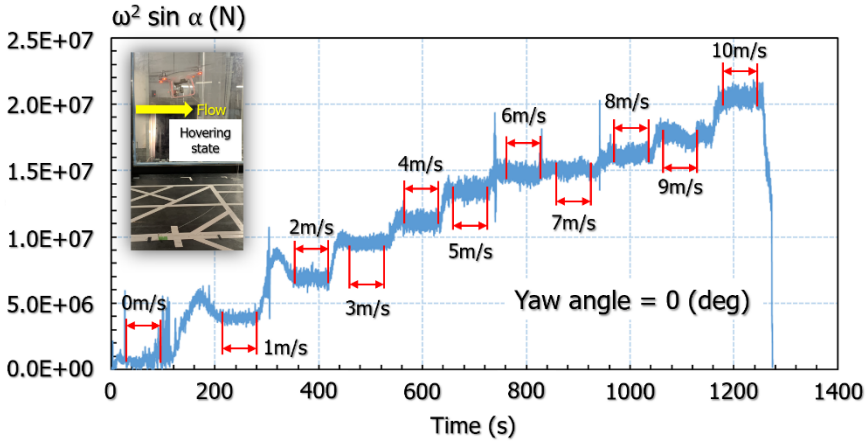

Figure 4. Time variation of $\omega^2 \sin\alpha$

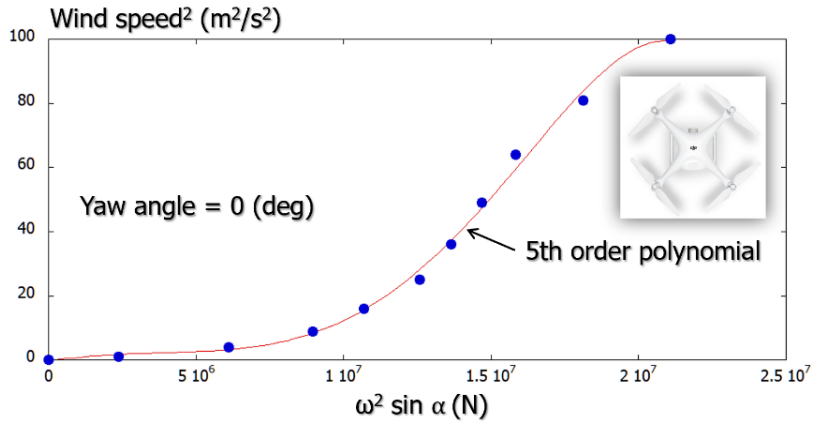

Figure 5. Calibration curve obtained in this study, DJI Phantom 4 Advanced

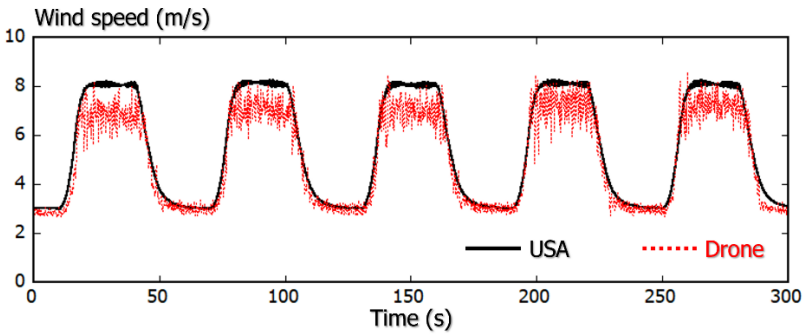

Figure 6. Measurement result using a drone targeting pulsating flow

4. Field measurements in the wake of the utility-scale wind turbine using drone

In this study, we attempted to measure airflow, using a drone, within the wake region of the wind power generation facility (3.3MW wind turbine manufactured by Vestas) in the Hibikinada area of Kitakyushu City, Fukuoka Prefecture, owned by Hibikinada Wind Energy Research Park LLC, shown in Figure 7. Figure 8 shows the airflow measurement points conducted in this study. Note that the x-axis changes with the nacelle. Table.1 shows the details of the airflow measurements carried out in this study. On the days when the experiment was conducted (2020.12.17 and 2020.12.25), the wind (westerly to northwesterly) was blowing steadily at an average speed of 7.0m/s.

What is noteworthy here is that we used two drones to constantly monitor the wind speed flowing into the wind turbine (x/D = -0.5) while measuring the airflow at tip (x/D = +0.25) and wake (x/D = +1.0) at the mid-span section (y = 0) passing through the wind turbine. Here, D means the rotor diameter of the wind turbine (=112m). The airflow measurement by the drone is for 10 minutes, and the time resolution is 0.1s. Here, we only show the results of run1 in table.1.

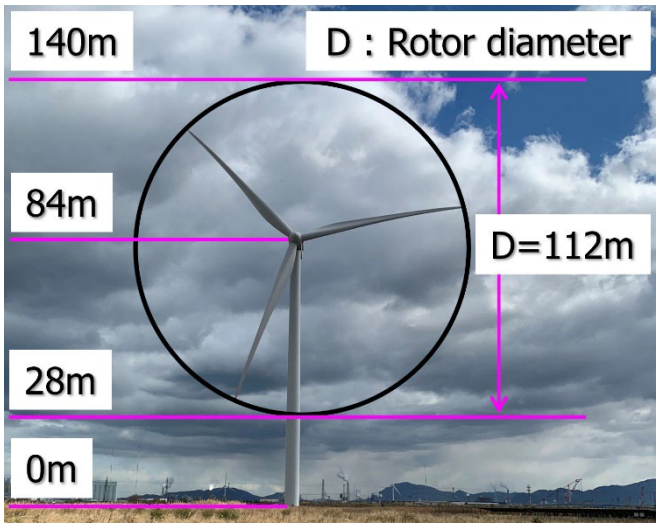

Figure 7. Utility-scale wind turbine used in this study, 3.3MW manufactured by Vestas

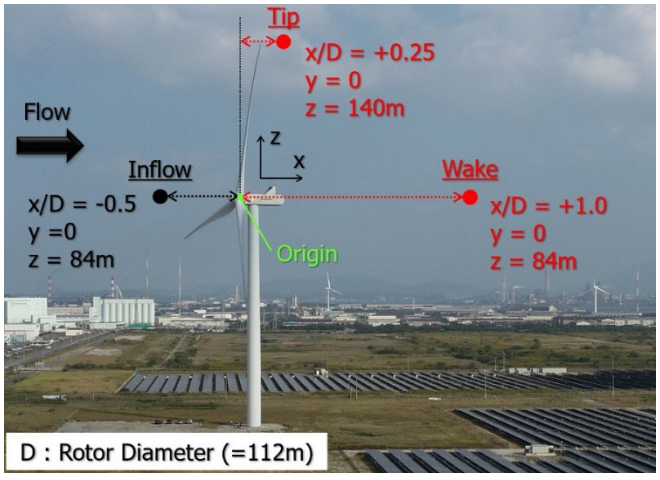

Figure 8. Airflow measurement points in this study

Table.1 Airflow measurements conducted in this study

	First drone	Second drone
run 1 (wake) 2020.12.17, 13:40～(JST)	x/D = -0.5 y =0 z = 84m	x/D = +1.0 y = 0 z = 84m
run 2 (tip) 2020.12.25, 13:35～(JST)		x/D = +0.25 y = 0 z = 140m

Figure 9 shows the actual measurement situation of Run 1 (Wake) shown in Table.1. Both visual observation at the site and flight record data confirmed that the drone was hovering stably at a predetermined position (altitude).

Figure 10 shows the temporal change in wind speed obtained by a drone during run 1 (wake). As already explained, the temporal resolution of airflow measurement by the drone is the same as before (0.1s). In this study, we focused on determining whether the drone itself can be used as an airflow sensor and understanding the airflow properties in the low frequency range within the wake region formed due to the rotation of the wind turbine blades, so we created Figure 10 by performing a 1.0s moving average operation. The solid black line is the measurement result at the upstream position of the wind turbine (x/D = -0.5), and the average wind speed for 10 minutes was approximately 7.2m/s as shown in the figure. In contrast, the solid red line is the measurement result within the wake region (x/D = +1.0). The average wind speed for 10 minutes was approximately 3.0m/s, which was significantly lower than the wind speed upstream of the wind turbine. This demonstrated that measurements using a drone can detect wake phenomena.

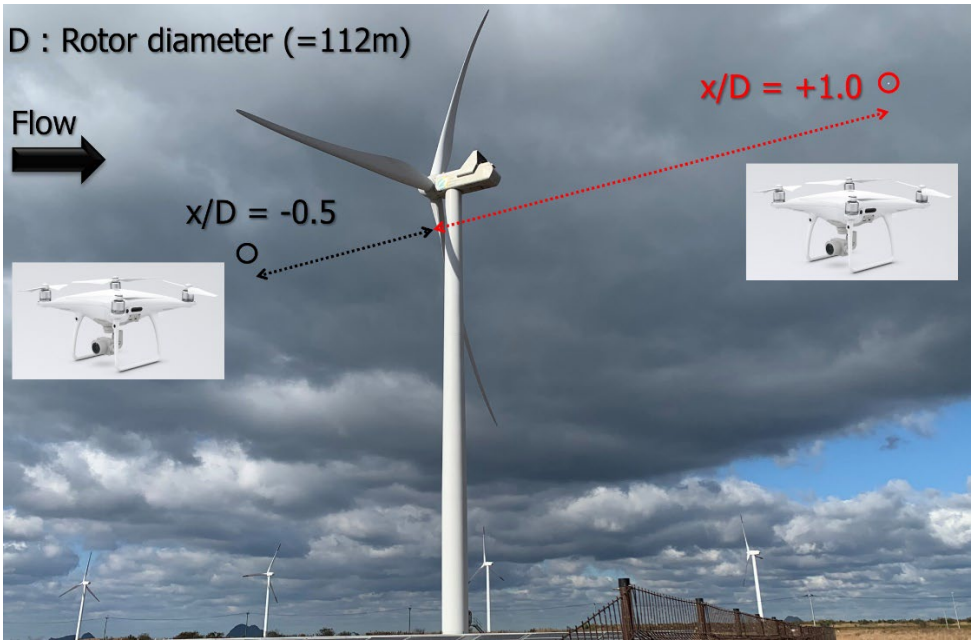

Figure 9. Drone hovering upstream (x/D = -0.5) and downstream (x/D = +1.0) of the wind turbine, run 1 (wake)

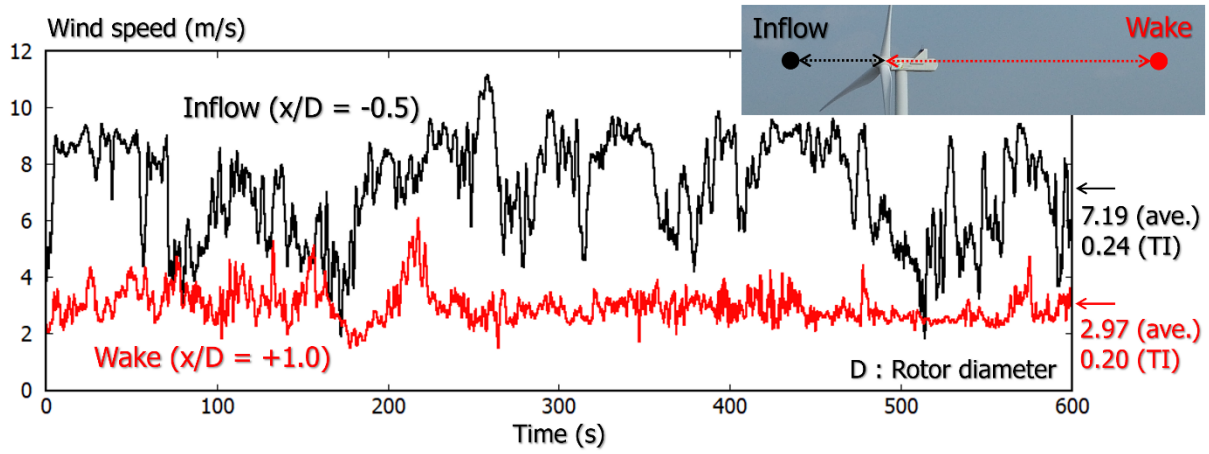

Figure 10. Temporal change in wind speed obtained by drone, results of run 1 (wake)

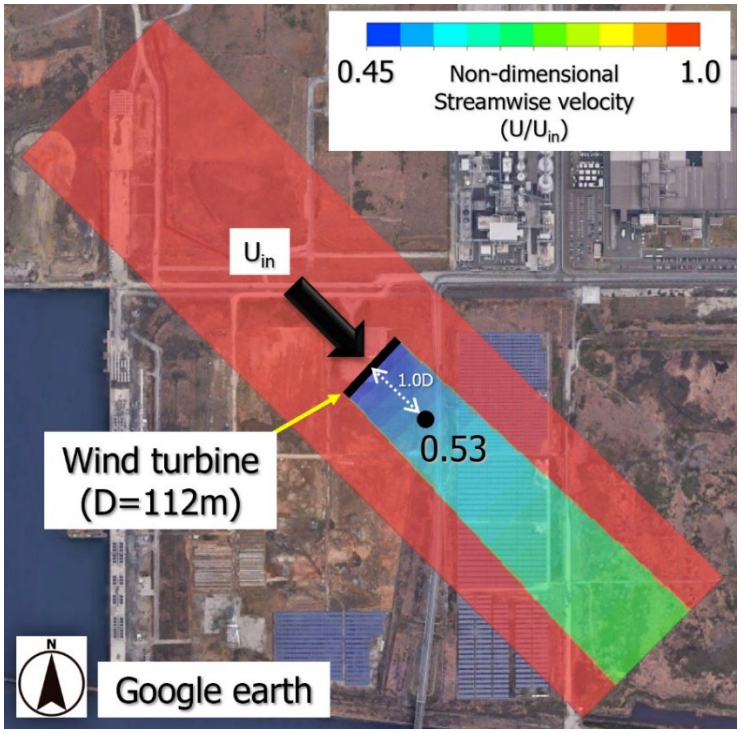

Figure 11. Wind turbine wake region reproduced by Park model
(thrust coefficient 0.8, diffusion coefficient 0.04)

In order to confirm the validity of the wind speed values within the wake region (x/D = +1.0) obtained by the drone, we compared them with the results of the Park model [4]), which is one of the engineering wake models (Fig. 11). When the wind speed in the wake area is normalized by the inflow wind speed, it becomes 2.97/7.19 = 0.41 for this drone measurement. On the other hand, the Park model had a value of 0.53. In the future, we plan to compare our results with the Cumulative-Curl (CC) wake model [5] that offers enhanced accuracy in near-wake predictions.

Figure 12 shows the results of spectrum analysis (FFT) for the temporal change in wind speed shown in Figure 10. Pay attention to the results for the upstream position of the wind turbine, shown by the solid black line. Since a moving average operation (1.0s) was performed, it was not possible to consider the high frequency range above 0.5Hz, but when we focused on around 0.1Hz, it became clear that a slope similar to the 2/3 power law was obtained. On the other hand, the results in the wake region (x/D = +1.0, near wake region) shown in red are different from the results for the upstream position of the wind turbine, and an increase in the power spectrum was confirmed in the range of 0.1 to 0.5Hz.

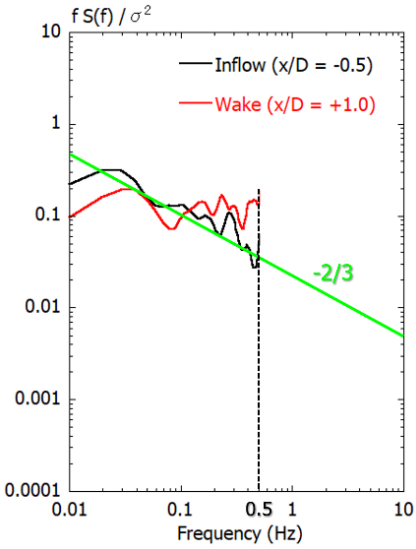

Figure 12. Results of spectral analysis (FFT)
on the temporal change in wind speed shown in Figure 10.

5. Conclusion

In this study, we investigated a method of utilizing the drone itself as a wind speed sensor without mounting a special observation device on the drone. The present method seems indeed promising but requires further validation. We plan to continue using observation masts, vertical lidar, etc. to understand and quantify wind speed measurement errors caused by drone hovering performance (positional accuracy and position change). In parallel with this, we plan to attempt area-wide measurements using multiple drones.

References

[1] Palomaki, R. T., Rose, N. T., van den Bossche, M., Sherman, T. J., & De Wekker, S. F. J., Wind Estimation in the Lower Atmosphere Using Multirotor Aircraft, Journal of Atmospheric and Oceanic Technology, 34(5), pp.1183-1191, 2017
[2] Akihiro Honda, Takeshi Kubota, Nanako Sasanuma, Ellena Otsuki, Flow visualization around an actual wind turbine using snow, Proceedings of Grand Renewable Energy 2022 International Conference, 71-74, 2022.12
[3] Hong, J., Toloui, M., Chamorro, L. et al., Natural snowfall reveals large-scale flow structures in the wake of a 2.5-MW wind turbine. Nat Commun 5, 4216, 2014
[4] Jensen, N.O., A Note on Wind Generator Interaction; Technical Report Risoe-M-2411(EN); Risø National Laboratory: Roskilde, Denmark, 1983
[5] Bay CJ, Fleming P, Doekemeijer B, King J, Churchfield M and Mudafort R, Addressing deep array effects and impacts to wake steering with the cumulative-curl wake model, Preprint WES-2022-17